Original Article

PROGRESS in MEDICAL PHYSICS 27(4), Dec. 2016
https://doi.org/10.14316/pmp.2016.27.4.224
pISSN 2508-4445, eISSN 2508-4453

Comparison of Temperature Distribution in Agar Phantom and Gel Bolus Phantom by Radiofrequency Hyperthermia

Dong Kyung Jung*, Sung Kyu Kim†, Joon Ha Lee‡, Sang Mo Youn*,
Hyung Dong Kim*, Se An Oh§, Jae Won Park†, Ji Won Yea†

*Department of Radiation Oncology, Daegu Fatima Hospital,
†Departments of Radiation Oncology, Yeungnam University College of Medicine,
‡Department of Biochemistry & Molecular Biology, Yeungnam University College of Medicine,
§Department of Radiation Oncology, Yeungnam University Medical Center, Daegu, Korea

The usefulness of Gel Bolus phantom was investigated by comparing the temperature distribution characteristic of the agar phantom produced to investigate the dose distribution characteristic of radiofrequency hyperthermia device with that of the Gel Bolus phantom under conditions similar to those of an agar phantom that can continuously carry out temperature measurement. The temperatures of the agar phantom and the Gel Bolus phantom were raised to 36.5±3°C and a temperature sensing was inserted at depths of 5, 10, and 15 cm from the phantom central axis. The temperature increase rate and the coefficient of determination were analyzed while applying output powers of 100 W and 150 W, respectively, at intervals of 1 min for 60 min under conditions where the indoor temperature was in the range 24.5～27.5°C, humidity was 35～40%, internal cooling temperature of the electrode was 20°C, size of the upper electrode was 250 mm, and the size of the lower electrode was 250 mm. The coefficients of determination of 150 W output power at the depth point of 5 cm from the central axis of the phantom were analyzed to be 0.9946 and 0.9926 in the agar and Gel Bolus phantoms, respectively; moreover, the temperature change equation of the agar and Gel Bolus phantoms with time can be expressed as follows in the state the phantom temperature is raised to 36°C: Y(G) is equation of Gel Bolus phantoms (in 5 cm depth) applying output power of 150 W. Y(G)=0.157X＋36. It can be seen that if the temperature is measured in this case, the Gel Bolus phantom value can be converted to the measured value of the agar phantom. As a result of comparing the temperature distribution characteristics of the agar phantom of a human-body-equivalent material with those of the Gel Bolus phantom that can be continuously used, the usefulness of Gel Bolus phantom was exhibited.

Key Words: Ratio frequency hyperthermia device, dose distribution characteristic, agar phantom, and Gel Bolus phantom

Introduction

As cancer incidence rate increases every year due to genetic and environmental factors, various cancer treatment methods are also gaining interests. The various approaches to treat cancers include surgery, anti-cancer therapy, and radiotherapy.[1,2] However, cancer cells cannot be completely removed by surgery; moreover, if cancer has metastasized to other organs, radiation is to be applied, in which case, normal tissues are inevitably damaged by the radiation. The method of treating cancer by administering anti-cancer drugs causes a side effect of damaging normal tissues. Recently, radiofrequency hyperthermia as a cancer treatment method that does not damage normal tissues while destroying cancer cells is gaining interest. As it maintains the normal tissues of the human body by minimizing the side effect on the cells and tissues inside human body while focusing on damaging cancer cells, it is widely used in clinical treatment.[3] It is based on the principle that human tis-

Received 16 December 2016, Revised 0 000 2016, Accepted 0 000 2016

Correspondence: Sung Kyu Kim (skkim3@ynu.ac.kr)
Tel: 82-53-620-3373, Fax: 82-53-624-3599

sues sensitive to heat, such as those affected by cancer, are easily damaged when exposed to a temperature of 42.5°C or higher. The advantage of hyperthermia is that the treatment efficiency is increased by 1.1 to 6.14 times without causing any side effects on patients with diverse types of cancers.[4-7] As radiofrequency hyperthermia is used directly on the affected area, it is essential to manage the accuracy of the radiofrequency hyperthermia device. While applying a radiofrequency hyperthermia device clinically, a hyperthermia plan for the treatment of cancer should be established, and measurement of the actual temperature inside the hyperthermia should be performed regularly to efficiently transfer thermal energy to the cancer cells. Currently, in clinical applications, the temperature rise and distribution of a radiofrequency hyperthermia device are measured using an agar phantom, a human-body-equivalent material. However, as agar phantom is vulnerable to long-term preservation, a new phantom, Gel Bolus phantom, was produced by comparing its temperature distribution characteristics with those of the existing agar phantom. This new Gel Bolus phantom can be used for the hyperthermia device. The temperature distribution characteristic of the Gel Bolus phantom was also studied.

Materials and Methods

Celsius TCS, Celsius42+ GmbH (Celsius, Germany) in the radiofrequency hyperthermia device, and, to measure the temperature of the produced "Gel Bolus phantom", Tempsens (TMS-G4-10-100SCA-M2-C42, Canada), a thermometer, and a temperature sensor (OTG-MPK5, Canada) were used. Moreover, powder agar CAR-15 (MSC Co., Korea) was used to produce agar phantom and super flex bolus (BOL-X II, USA) was used

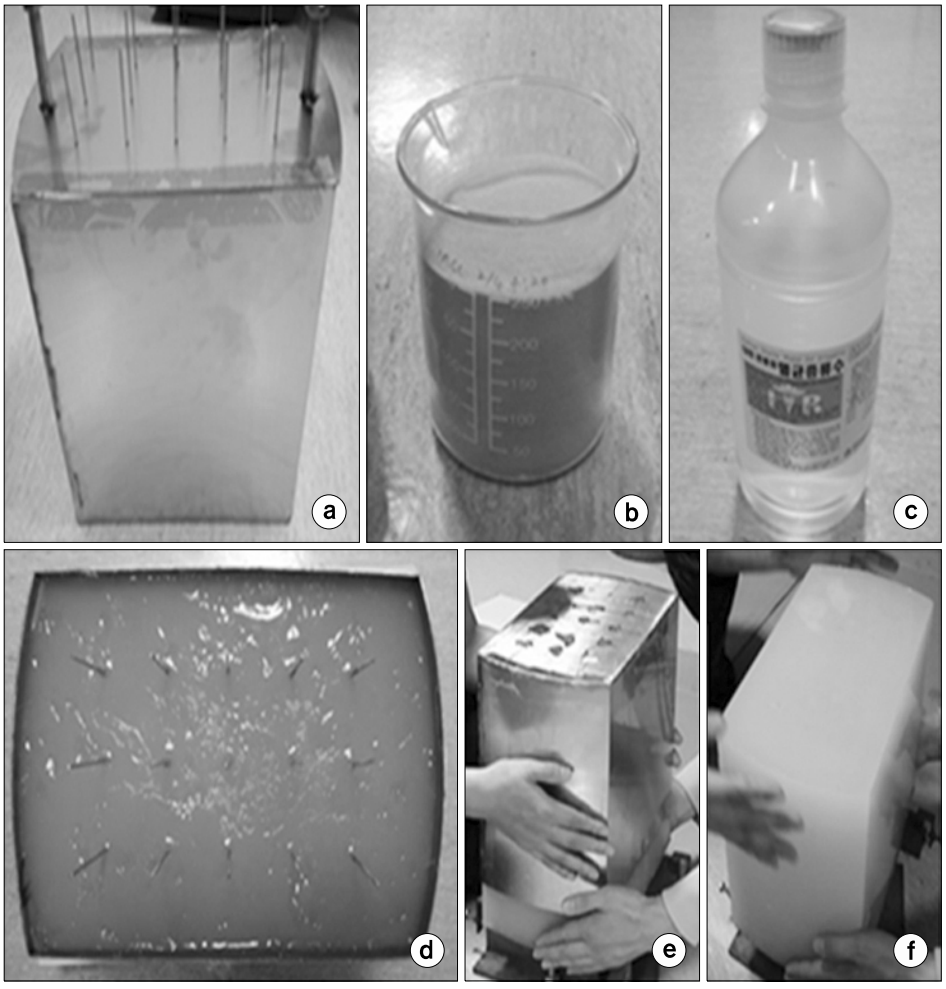

Fig. 1. Making of agar phantom: (a) Agar phantom mold, (b) Agar powder of MSC Co. Ltd, (c) Sterile water, (d) Gel agar solidified with phantom, (e) Gel agar phantom separated from the mold, (f) Completed production of agar phantom.

to produce the Gel Bolus.

1. Production of agar phantom

To produce an agar phantom in the form of the lower abdomen of a human body, an agar phantom mold in the size of 300×300×200 mm was produced using 2-mm-thick austenitic stainless steel KS STS304, and a mixture of 100 ml powder agar and 19,000 ml sterile distilled water was poured into the mold and separated from it after a 24-h solidification process (Fig. 1).

2. Production of Gel Bolus phantom

A human-body-equivalent material, which is chemically composed of elements such as carbon, oxygen, hydrogen, and phosphorus, and with a specific gravity similar to that of water (density of 1.03 g/cm^3), was banked up to 200 mm. The height of the Gel Bolus was same as that of the agar phantom, so as to not allow the generation of any air layer between the surfaces of the bolus (Fig. 2).

3. Measurement of temperature distribution at depth points

The temperatures of the agar and Gel Bolus phantoms were raised to 36.5±3°C, and a temperature sensor was inserted at the depths of 5, 10, and 15 cm from the phantom central axis. The rate of temperature increase and the coefficient of determination were analyzed while applying output powers of 100 W and 150 W, respectively, at intervals of 1 min for 60 min under conditions where the indoor temperature was in the range 24.5～27.5°C, humidity was 35～40%, internal cooling temperature of the electrode was 20°C, size of the upper electrode was 250 mm, and the size of the lower electrode was 250 mm (Figs. 3 and 4).

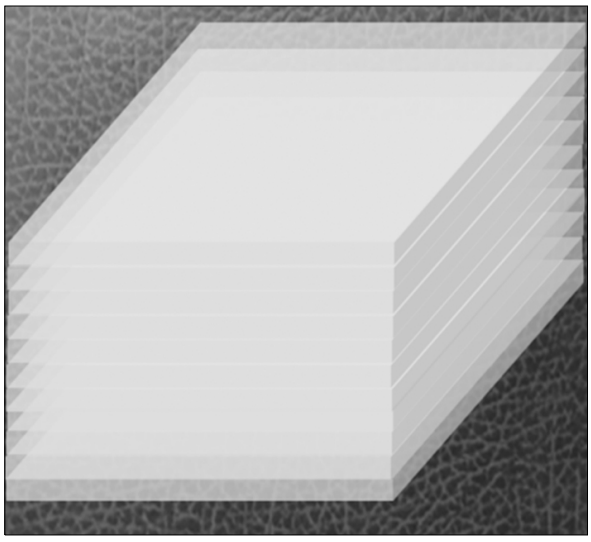

Fig. 2. Gel bolus phantom.

Result

1. Temperature distribution in the agar phantom

The analysis of the temperature change of 360 kJ at depth points with the output power of 100 W applied for 60 min indicated that the coefficients of determination were 0.9946, 0.9835, and 0.9949 at depths of 5, 10, and 15 cm, respectively. In addition, the temperature of the agar phantom rose by 1°C at 9.06, 10.95, and 9.94 min at depths of 5, 10, and 15 cm from the phantom central axis, respectively (Fig. 5).

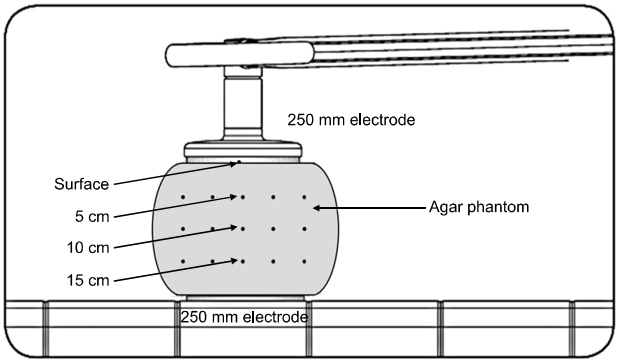

Fig. 3. Illustration of the simulation model on the agar phantom.

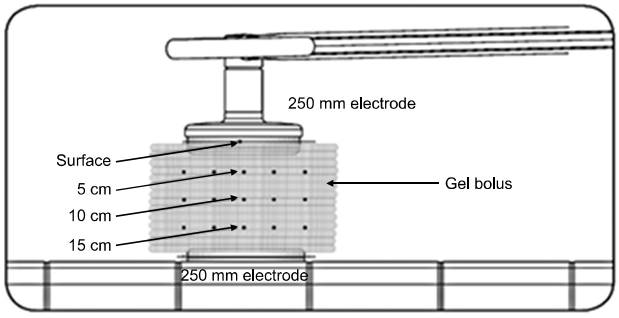

Fig. 4. Illustration of the simulation model on the gel bolus phantom.

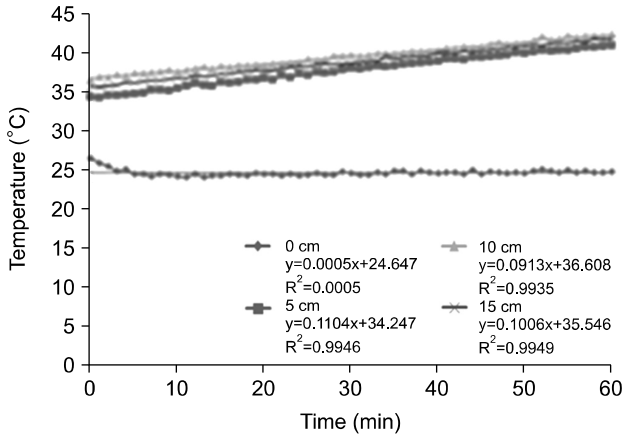

Fig. 5. Depth of measurement temperature on the agar phantom for 60 min at 100 W output power.

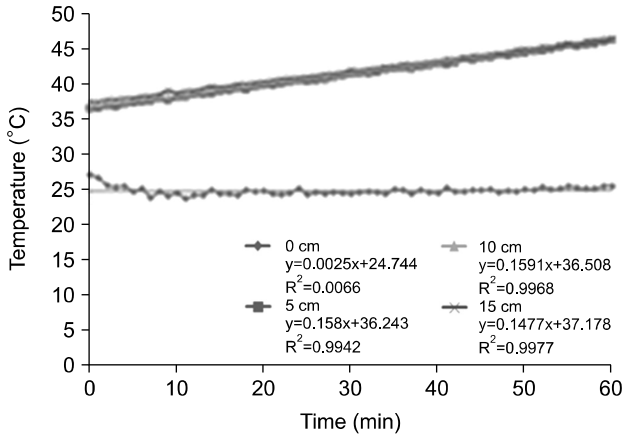

Fig. 6. Depth of measurement temperature on the agar phantom for 60 min at 150 W output power.

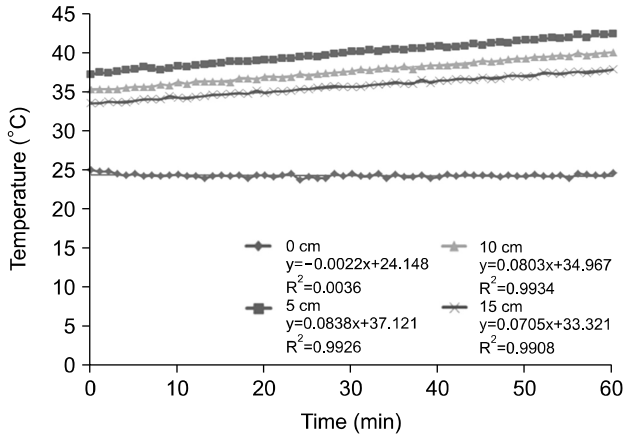

Fig. 7. Depth of measurement temperature on the gel bolus phantom for 60 min at 100 W output power.

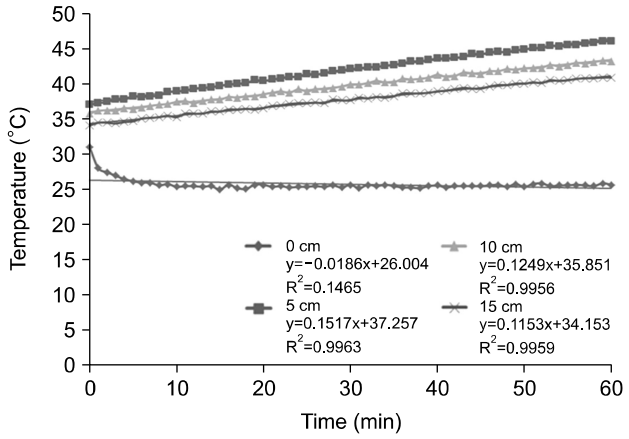

Fig. 8. Depth of measurement temperature on gel bolus phantom for 60 min at 150 W output power.

The analysis of the temperature change of 540 kJ at depth points with the output power of 150 W applied for 60 min indicated that the coefficients of determination were 0.9982, 0.9968, and 0.9977 at depths of 5, 10, and 15 cm, respectively. In addition, temperature of the agar phantom rose by 1°C at 6.33, 6.29, and 6.77 min at depths of 5, 10, and 15 cm from the phantom central axis, respectively (Fig. 6).

2. Temperature distribution in the Gel Bolus phantom

The analysis of the temperature change of 360 kJ at depth points with the output power of 100 W applied for 60 min indicated that the coefficients of determination were 0.9926, 0.9934, and 0.9908 at depths of 5, 10, and 15 cm, respectively. In addition, the temperature of the agar phantom rose by 1°C at 11.93, 12.45, and 14.18 min at depths of 5, 10, and 15 cm from the phantom central axis, respectively (Fig. 7).

of the analysis of the temperature change of 540 kJ at deep points with the output power of 150 W applied for 60 min indicated that the coefficients of determination were 0.9963, 0.9956, and 0.9959 at depths of 5, 10, and 15 cm, respectively. In addition, the temperature of the agar phantom rose by 1°C at 6.59, 8.01, and 8.67 min at depths of 5, 10, and 15 cm from the phantom central axis, respectively (Fig. 8).

3. Comparative analysis of the temperatures measured in the agar and Gel Bolus phantoms

1) Comparison of the temperatures measured at 5-cm depth with 100 W output power: The coefficients of determination obtained with 100 W output power at the depth of 5 cm from the phantom central axis were 0.9946 in the agar phantom and 0.9926 in the Gel Bolus phantom, and the time taken for a temperature increase of 1°C in the Gel Bolus phantom was analyzed to be 11.93 min, which was 2.87 min longer than 9.06 min, the time taken in the agar phantom. The temperature rise gradients of the agar and Gel Bolus phantoms were found to be 0.1104 and 0.0838, respectively (Fig. 9).

2) Comparison of the temperatures measured at 5-cm depth with 150 W output power: The coefficients of determination obtained with 150 W output power at the depth of 5 cm from the phantom central axis were 0.9982 in the agar phantom and 0.9963 in the Gel Bolus phantom, and the time taken for a temperature increase of 1°C in the Gel Bolus phantom was analyzed to be 6.59 min, which was 0.26 min longer than 6.33 min, the time taken in the agar phantom. The temperature rise gradients of the agar and Gel Bolus phantoms were found to be 0.158 and 0.1517, respectively (Fig. 10). The equations of temperature change with time of the agar and Gel Bolus phantoms can be expressed as follows in the state the phantom temperature is raised to 36°C:

$$Y(A)=0.158X+36 \quad (1)$$

$$Y(G)=0.157X+36 \quad (2)$$

Here, Y(A) is the agar phantom function, Y(G) is the Gel Bolus phantom function, and X represents time.

By comparing Equations (1) and (2), if the output is set to 150 W and the temperature is measured at 5-cm depth, the Gel Bolus phantom value can be converted to the measured value of the agar phantom.

3) Comparison of the temperatures measured at 10-cm depth with 100 W output power: The coefficients of determination obtained with 100 W output power at the depth of 10 cm from the phantom central axis were 0.9935 in the agar phantom and 0.9934 in the Gel Bolus phantom, and the time taken for a temperature increase of 1°C in the Gel Bolus phantom was analyzed to be 12.48 min, which was 1.53 min longer than 10.95 min, the time taken in the agar phantom. The temperature rise gradients of the agar and Gel Bolus phantoms were found to be 0.0913 and 0.0803, respectively (Fig. 11).

4) Comparison of the temperatures measured at 10-cm depth with 150 W output power: The coefficients of determination obtained with 150 W output power at the depth of 10 cm from the phantom central axis were 0.9967 in the agar phantom and 0.9956 in the Gel Bolus phantom, and the time taken for a temperature increase of 1°C in the Gel Bolus phantom was analyzed to be 8.01 min, which was 1.72

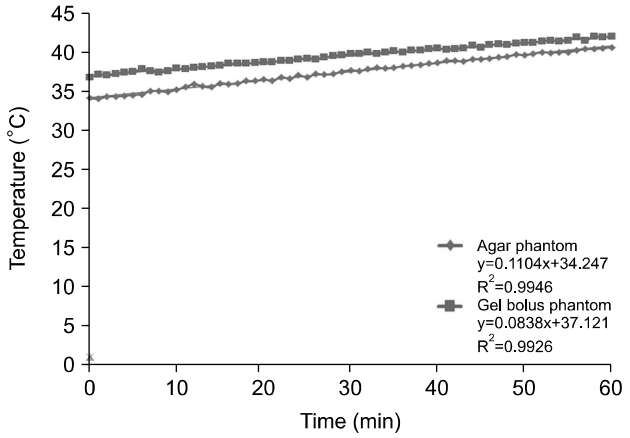

Fig. 9. 5-cm depth for 60 min at 100 W output power for the temperature analysis of the agar and gel bolus phantoms.

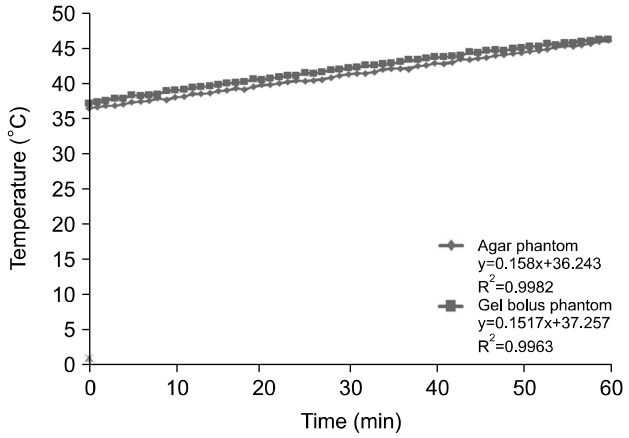

Fig. 10. 5-cm depth for 60 min at 150 W output power for the temperature analysis of the agar and gel bolus phantoms.

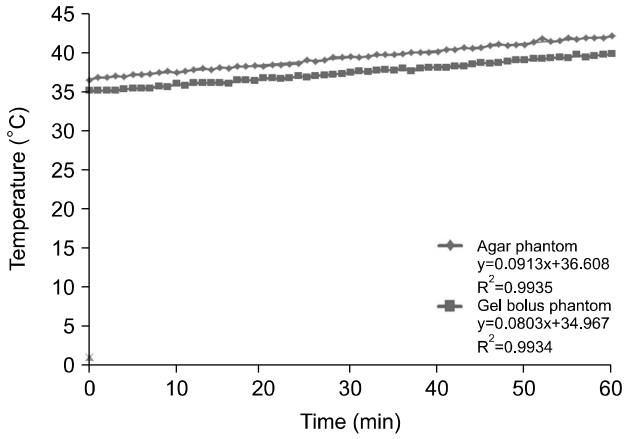

Fig. 11. 10-cm depth for 60 min at 100 W output power for the temperature analysis of the agar and gel bolus phantoms.

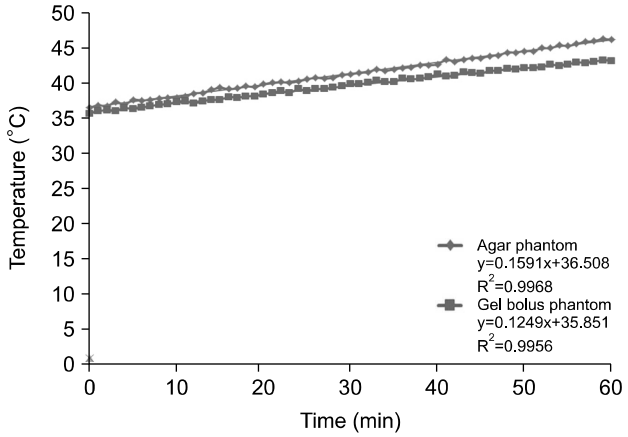

Fig. 12. 10-cm depth for 60 min at 150 W output power for the temperature analysis of the agar and gel bolus phantoms.

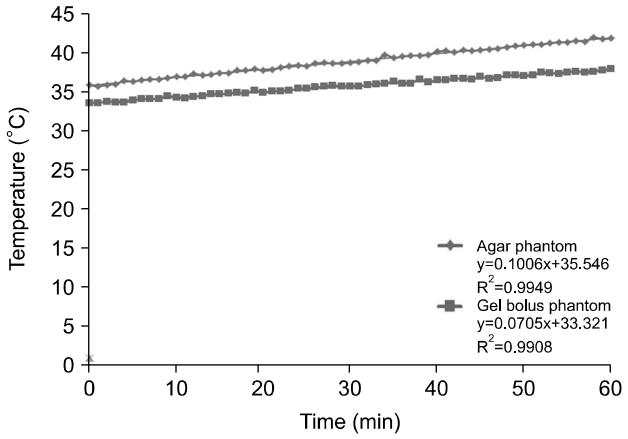

Fig. 13. 15-cm depth for 60 min at 100 W output power for the temperature analysis of the agar and gel bolus phantoms.

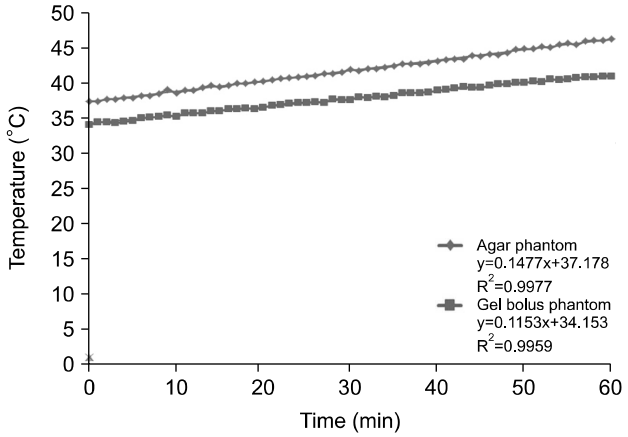

Fig. 14. 15-cm depth for 60 min at 150 W output power for the temperature analysis of the agar and gel bolus phantoms.

min longer than 6.29 min, the time taken in the agar phantom. The temperature rise gradients of the agar and Gel Bolus phantoms were found to be 0.1591 and 0.1249, respectively (Fig. 12).

5) Comparison of the temperatures measured at 15-cm depth with 100 W output power: The coefficients of determination obtained with 100 W output power at the depth of 15 cm from the phantom central axis were 0.9949 in the agar phantom and 0.9908 in the Gel Bolus phantom, and the time taken for a temperature increase of 1°C in the Gel Bolus phantom was analyzed to be 14.18 min, which was 4.24 min longer than 9.94 min, the time taken in the agar phantom. The temperature rise gradients of the agar and Gel Bolus phantoms were found to be 0.1006 and 0.0705, respectively (Fig. 13).

6) Comparison of the temperatures measured at 15-cm depth with 150 W output power: The coefficients of determination obtained with 150 W output power at the depth of 10 cm from the phantom central axis were 0.9977 in the agar phantom and 0.9956 in the Gel Bolus phantom, and the time taken for a temperature increase of 1°C in the Gel Bolus phantom was analyzed to be 8.67 min, which was 1.9 min longer than 6.77 minutes, the time taken in the agar phantom. The temperature rise gradients of the agar and Gel Bolus phantoms were found to be 0.1477 and 0.1153, respectively (Fig. 14).

Discussion and Conclusion

The comparison of the permittivity of the two phantoms resulting from their material properties can enable us to derive appropriate equations. Owing to the time it takes to produce an agar phantom, it is impossible to use the agar phantom if the temperature is required to be measured suddenly for accuracy management of a hyperthermia device. However, as a Gel Bolus phantom can measure the temperature of a hyperthermia device immediately in an emergency, it is assumed to be feasible as a substitutive phantom if the temperature is measured at a depth of 5 cm using with 150 W output power.

For cancer treatment, surgery, anti-cancer therapy, radiotherapy, and hyperthermia are employed. Among these, as hyperthermia causes less damage to normal tissues than when treated with radiotherapy and the radiation chemistry therapy, it has become an acceptable approach in the cancer treatment field.[8,9] As new blood vessels of cancer cells have more impaired blood flow than normal blood vessels, they are easily destroyed when a temperature increase is induced, because the vascular system cannot be maintained.[10,11] Moreover, if hyperthermia is carried out parallel with the oxygen regeneration effect, the treatment effect can be enhanced by increasing the chemosensitivity to cancer tissues.[12,13] A radiofrequency hyperthermia device effectively transfers thermal energy to cancer cells. However, as a radiofrequency hyperthermia device is directly used on the affected area, it is essential to manage the accuracy of temperature change. In this study, the agar used to develop the human body model phantom is a material that is frequently used by bionics researchers as it is composed of a human-body-equivalent material having a physical characteristic where the shape can be easily changed.[14,15] However, agar phantom biologically allows bacteria such as mildew to easily reproduce. Accordingly, the temperature was measured using the Gel Bolus phantom, also composed of a human-body-equivalent material used for radiation oncology. The coefficients of determination of the agar phantom when the output powers were 100 W and 150 W were found to be between 0.9935 and 0.9982, and those of the Gel Bolus phantom were between 0.9926 and 0.9956, respectively, which are shown to be close to 1. Further, it was observed that the time taken for a temperature rise lengthened by 2.87 min when the output was 100 W and 1.29 min when the output was 150 W. The temperature rise gradient correction factor of the Gel Bolus phantom was between 1.137 and 1.427 when the output power was 100 W and between 1.042 and 1.281 when the output power was 150 W.

Through this study, the temperature distribution of a radiofrequency hyperthermia device could be determined using the proportional index and the time taken for temperature rise when an agar phantom and a newly produced Gel Bolus phantom, both composed of human-body-equivalent materials, were appropriately used. It showed the usefulness of the Gel Bolus phantom.

References

1. Byun YJ, Lee EH, Lee JP, Chang KH, Ryu HS: The effect of hormone replacement therapy on osteoporosis following irradiation of gynecologic cancer patients. J Gynecol Oncol 16(1): 53-60 (2005)
2. Chung IY, Kim EJ, Park JM, Yoo JM: Results of combined chemotherapy and radiotherapy for advanced intraocular retinoblastoma, Korean J Ophthalmol 44(7): 1528-1537 (2003)
3. Kim MO: Concurrent chemoradiotherapy of locally advanced pancreatic carcinoma and effects of hyperthermia. Korean Cancer Association 26(4): 561-566 (1994)
4. Cui ZG, Piao JL, Rehman MU, Ogawa R, Li P, Zhao QL, et al: Molecular mechanisms of hyperthermia-induced apoptosis enhanced by withaferin A. Eur J Pharmacol 15(723): 99-107 (2014)
5. Hatashita M, Taniguchi M, Baba K, Koshiba K, Sato T, Jujo Y, et al: Sinodielide A exerts thermosensitizing effects and induces apoptosis and G2/M cell cycle arrest in DU145 human prostate cancer cells via the Ras/Raf/MAPK and PI3K/Akt signaling pathways. Int J Mol Med 33(2): 406-414 (2014)
6. Song X, Kim SY, Lee YJ: Evidence for two modes of synergistic induction of apoptosis by mapatumumab and oxaliplatin in combination with hyperthermia in human colon cancer cells. PLoS One 8(8): e73654 (2013)
7. Jiang W, Bian L, Wang N, He Y: Proteomic analysis of protein expression profiles during hyperthermia-induced apoptosis in Tca8113 cells. Oncol Lett 6(1): 135-143 (2013)
8. Jang HS: Clinical trial of concomitant thermo-chemotherapy in cervix cancer patients. Korean Cancer Association 27(6): 968-977 (1995)
9. Suh CO, Loh JK, Seong JS, Roh JK, Kim BS, Park IS, et al: Effect of radiofrequency hyperthermia on hepatocellular carcinoma. Korean Cancer Association 20(2): 117-125 (1988)
10. Solopan S, Belous A, Yelenich A, Bubnovskaya L, Kovelskaya A, Podoltsev A, et al: Lanthanum-strontium

manganite magnetic fluid as potential inducer of tumor hyperthermia. Exp Oncol 33(3): 130-135 (2011)
11. **Lui PC, Fan YS, Xu G, Ngai CY, Fung KP, Tse GM, et al**: Apoptotic and necrotic effects of tumour necrosis factor-alpha potentiated with hyperthermia on L929 and tumour necrosis factor-alpha-resistant L929. Int J Hyperthermia 26(6): 556-564 (2010)
12. **Thews O, Lambert C, Kelleher DK, Biesalski HK, Vaupel P, Frank J**: Impact of therapeutically induced reactive oxygen species and radical scavenging by alpha-tocopherol on tumor cell adhesion. Oncol Rep 18(4): 965-971 (2007)
13. **Ahmed K, Zhao QL, Matsuya Y, Yu DY, Salunga TL, Nemoto H, et al**: Enhancement of macrosphelide-induced apoptosis by mild hyperthermia. Int J Hyperthermia 23(4): 353-361 (2007)
14. **Sikora M, Gese A, Czypicki R, Gąsior M, Tretyn A, Chojnowski J, et al**: Correlations between polymorphisms in genes coding elements of dopaminergic pathways and body mass index in overweight and obese women. Endokrynol Pol 64(2): 101-107 (2013)
15. **Frascione N, Pinto V, Daniel B**: Development of a biosensor for human blood: new routes to body fluid identification. Anal Bioanal Chem 404(1): 23-28 (2012)